EDGE CRACK DETECTION: A THEORETICAL AND EXPERIMENTAL STUDY

D. Lehther, J. Chao, N. Nakagawa, and J. C. Moulder
Center for Nondestructive Evaluation
Iowa State University
Ames, IA 50011

INTRODUCTION

Detection of cracks close to an edge by conventional eddy current techniques is difficult, owing to the significant background signal from the edge. It is necessary to develop methods for minimizing the effect of the background signal, thereby increasing the probability of detection. The edge signal is known to be influenced by a number of factors and it is essential to characterize these in order to minimize its influence. This study aims at developing a good understanding of these factors so as to facilitate the development of such techniques. A boundary element method (BEM) approach was used to model the signal due to the edge and to compare with experimental measurements. Experiments were conducted on electro-discharge machined (EDM) slots in the vicinity of an edge using both absolute and differential probes. The influence of orientation of a differential probe on the signal from the crack and the edge was also studied . We report on the development of improved methods to reduce the influence of signal due to the edge by appropriate use of differential probes and with the aid of signal processing. An inexpensive physical technique which results in a improved detectability was also developed .

THEORY

The boundary element method (BEM) based model is formulated using the newly developed extended magnetic potential (EMP) approach [1]. This formulation has proven to be very effective in modeling specimens with geometrical singularities (e.g. edges) without any special treatment. On the other hand, the more conventional Stratton-Chu formulation requires special treatment at geometrical singularities in order to obtain the correct solution. Readers should refer to [2] for a more detailed discussion on this issue. The EMP approach uses a magnetic scalar potential as the unknown function in the air region. In the traditional potential approach, the total magnetic field in the air region is defined as only the gradient of a scalar potential function. However, in the EMP approach the total magnetic field in the air region is defined to be the sum of the gradient of the potential and the H-field produced by the coil in the absence of the specimen. Using this formulation, we avoid the multi-valuedness problem associated with the scalar potential function. Therefore,

$$\vec{H} = \vec{H}^{(0)} + \nabla\psi \qquad (1)$$

Review of Progress in Quantitative Nondestructive Evaluation, Vol. 15
Edited by D.O. Thompson and D.E. Chimenti, Plenum Press, New York, 1996

where

$\vec{H}^{(0)}$ is the incident field in the absence of the specimen and,
ψ is the scalar potential function.

The scalar potential is then extended into the metallic specimen region via continuity. Inside the metal, the total H-field is defined to be the sum of another scalar potential function and a auxiliary vector function,

$$\vec{H} = \vec{h} + \nabla\Psi \tag{2}$$

with the interface conditions

$$\hat{n} \times \vec{h} = \hat{n} \times \vec{H}^{(0)} \tag{3}$$

$$\psi = \Psi \tag{4}$$

where $\hat{n}$ is an unit normal on the specimen surface pointing towards the air region.

Consequently, the governing boundary integral equations are

$$-\tfrac{1}{2}\psi(p) - \int_S \left[-\tfrac{\partial G_0}{\partial n}\psi(q) + G_0\left(\tfrac{B_n(q)}{\mu_0} - H_n^{(0)}(q)\right)\right] dS_q = 0 \tag{5}$$

$$-\tfrac{1}{2}\psi(p) + \int_S \left[-\tfrac{\partial G}{\partial n}\psi(q) + G\left(\tfrac{B_n(q)}{\mu} - h_n(q)\right)\right] dS_q = 0 \tag{6}$$

$$-\tfrac{1}{2}\vec{h}(p) + \int_S \left[(\nabla G) \times (\hat{n} \times \vec{H}^{(0)}(q)) - (\nabla G) h_n - k^2 G\left(\tfrac{\hat{n} \times \vec{E}(q)}{j\omega\mu} - \hat{n}\psi(q)\right)\right] dS_q \tag{7}$$

where G_0 is the free-space static Green's function, G is the free-space dynamic Green's function associated with the metallic wavenumber k. By solving the unknowns h_n, B_n, and ψ on the specimen surface using the BEM, we can calculate either the E-field or the H-field everywhere in space. To calculate the impedance, we simply apply Auld's reciprocity theorem [3].

EXPERIMENTAL SETUP

The experiments described as a part of this work were performed on a multi-axis eddy-current scanning system. The motion of each axis is by means of stepper-motor control, which is interfaced to a PC through a General Purpose Interface Bus (GPIB) protocol. This setup is capable of executing eddy-current measurements on a general 3-D surface making use of its 5 degrees of freedom. The use a multi-axis system of this nature is to ensure that the eddy-current probe remains perpendicular to the surface at all times, thereby maintaining a constant air gap at all points of measurement. It is possible to use a either an *hp4149A* impedance analyzer or a commercial eddy-scope to make the impedance measurements with this setup. The system is capable of displaying the measured data values in real time.

The *hp4149A* impedance analyzer is also interfaced to the P.C by a GPIB protocol. The impedance analyzer can be configured to make measurements at a particular frequency, at a specific rate of averaging. The real and imaginary parts of the data are acquired remotely from the *hp4149A* via the GPIB interface. The data are stored on the PC for later analysis.

Some of the experiments described below were performed using a differential probe. A conventional eddy-scope was used to study the differential response of the probe. The output from the eddy-scope comprises two analog signals corresponding to the vertical and horizontal axis voltage of the eddy-scope. The analog signals were digitized using an analog to digital (A/D) conversion card and stored on the PC. The sampling of the analog signal can be controlled depending on the noise characteristics of the signal being acquired.

EXPERIMENTS

Edge Signal in Absence of a Flaw

A set of measurements were made on the edge of a rectangular block (1/2" x 3" x 3") of aluminum (Al 7075, $\sigma = 2.26 \times 10^7$ [S/m]). The probe motion was from the metal surface into the air, the direction of the probe motion being perpendicular to the edge. An air-cored absolute probe (L-Probe) was used in these measurements. The details of this probe are given in Table 1. The measurements were performed over a frequency range of 100 kHz to 1 MHz. The impedance change was compared with theoretical results. The details of variation of real and imaginary part of the signals and the comparison with theory are presented in the section on results.

Edges with Flaws

Two rectangular blocks of titanium (Ti-6Al-4V) with EDM notches close to the edge were used as part of this work. The first specimen has five EDM notches that start at a distance of 150 mils from the edge. All EDM notches are oriented perpendicular to the edge of the specimen. The length of the notches vary from 30 mils to 150 mils. The notch labeled 'A' breaks the edge and at the other extreme notch 'E' is at distance of 120 mils from the edge. The dimensions of the notches and their location with respect to the edge are as shown in Table 2. The block is designed in this fashion to simulate the effect of the growth of a crack towards the edge. The second block is identical to the first in terms of

Table 1. Characteristics of probe L.

Number of turns	235
Inductance in air (μH)	37.84
Resonant frequency (MHz)	3.89
Mean coil radius (mm)	0.81
Inside diameter (mm)	0.64
Outside diameter (mm)	2.6
Coil length (mm)	2.9

Table 2. Details of specimen with EDM notches

Specimen	Length (mils)	Width (mils)	Depth (mils)	Distance (mils)
A	150	4	15	0
B	120	4	15	30
C	90	4	15	60
D	60	4	15	90
E	30	4	15	120

dimensions. This block was used to study the feasibility of using a "backing-plate" to minimize the effect of the edge on eddy current signals.

Orientation of the Probe

The orientation of the probe has an influence on both the signal from the crack and the signal from the edge. This effect is due to the relative orientation of the differential coil pair with respect to the crack and the edge. The above mentioned specimen is interesting from this point of view, since the edge and the notches are mutually perpendicular. The measurements on the specimen were made in two orientations, "perpendicular" to the edge, (i.e., the coils move across the edge one after the other as the coil scans over the edge) and "parallel" to the edge (i.e., both the coils move across the edge at the same time).

Effect of a Backing Plate

The specimen was scanned with the backing plate placed along its edge. The physical implication of using a backing plate is that the effect of the edge is now reduced to the discontinuity between the specimen and the backing plate. The resultant effect of the edge and the notch signals were observed in both *parallel* and *perpendicular* probe orientations.

Signal Processing

The effect of the edge which forms the background signal of the composite signal obtained by a typical 2-D scan described above, was minimized using a software based signal processing technique. This signal processing procedure involves approximation of the background signal by using the 2-D scan data obtained from the scan and then subtracting the approximation of the background from the original signal.

RESULTS

The measurements performed on the straight edge of the aluminum block are shown in Figure 1.. The graphs show the variation in the real and imaginary part of the impedance of the probe as it moves from the metal surface into the air. The position "0.0" on the horizontal axis corresponds to the location of the edge.

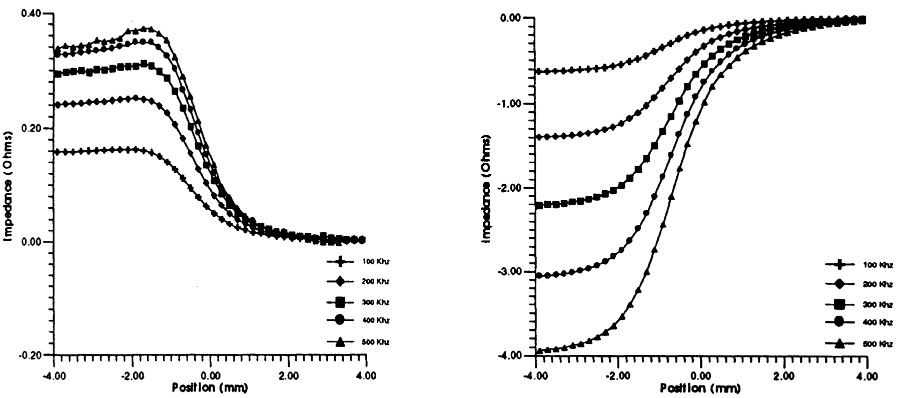

Real Part

Imaginary Part

Fig 1. Edge signal (100 kHz - 500 kHz).

The experimental data from the measurements were compared with theoretical calculations. The Dodd-Deeds solution gives the expected impedance change from metal to air. This is represented by a line indicating the change in impedance relative to impedance of the probe in air. The experimental results are also compared to BEM based model calculations by Chao and Nakagawa [2]. Both the Stratton-Chu and EMP formulations were tested. The comparison of impedance change at 100 kHz is illustrated in Fig. 2. It was observed that the theoretical predictions agree well with the experimental values of impedance for both real and imaginary parts for low frequencies (as is evident in the data for 100 kHz), but the impedance predictions by both models deviate from the experimental measurements at higher frequencies. The real part of the impedance exhibits a small peak, which becomes more pronounced at higher frequencies, as illustrated in Fig. 1. In the calculations, the results from the extended magnetic potential follow this behavior more closely than those calculated with the Stratton-Chu formulation. But at high frequencies, both models deviate from experiment. This is thought to be related to non-ideal probe behavior.

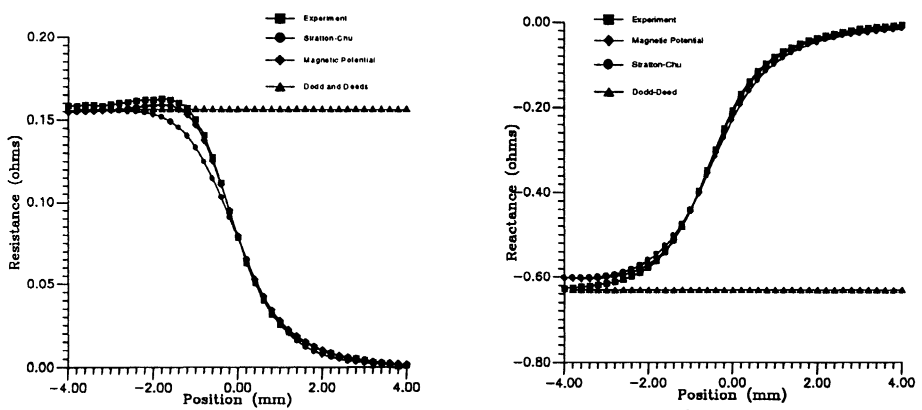

Real Part

Imaginary Part

Fig 2. Comparison of experiment with theory at 100 kHz.

Measurements of Edges with Flaws using Differential Probe

The vertical and horizontal channel outputs of the eddy scope for a 1-D scan over notches ‘A’ and ‘E’ are illustrated in Figs. 3 and 4. The signal due to a flaw typically resul in a figure-eight lissajous pattern and that due to the edge forms a relatively large open loop. Figure 4 illustrates the observation that the presence of an edge results in an incomplete figure-eight for the flaw. The influence of the edge in terms of the proximity to the edge is illustrated by these two notches, notch ‘E’ being farthest from the edge, whereas ‘A’ breaks the edge. The corresponding 2-D scans are shown in Figs.5 and 6.

Probe Orientation

The orientation of the two coils of the differential probe during the scan has a significant effect on the magnitude of the edge signal relative to the signal due to the edge. Figure 7 shows the data corresponding to notch ‘A’ with the scan performed in the parallel orientation, i.e., with a line drawn through the center of the two coils oriented parallel to the edge.. The signal due to the notch is comparable to that due to the edge. The signal from the same notch, however, is overshadowed by the edge signal in the case of the perpendicular orientation, as shown in Fig. 8.

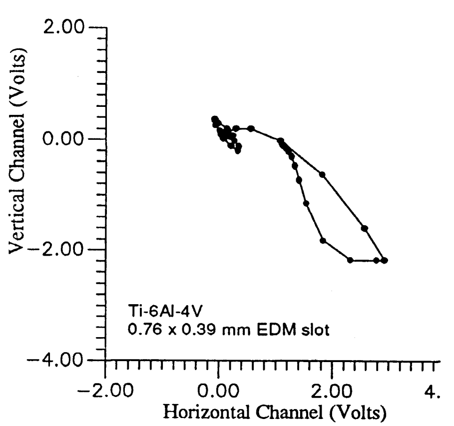

Fig 3. 1-D scan of notch ‘E.’

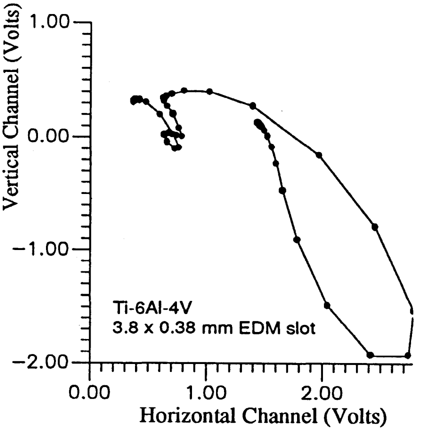

Fig 4. 1-D scan of notch ‘A.’

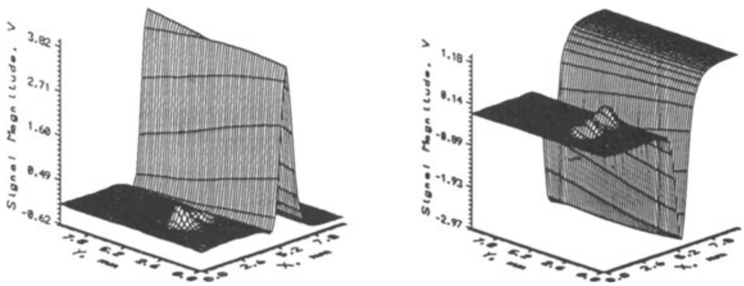

Horizontal Channel

Vertical Channel

Fig. 5. 2-D scan of notch ‘E’ with probe axis perpendicular to edge.

Effect Of Backing Plate

The scans performed with the backing plate in contact with the edge show a significant reduction in the effect due to the edge. Figure 7. shows a scan without the backing plate with the probe in the perpendicular orientation. Figure 10 shows the data obtained using a backing plate, with all else being equal.

Signal Processing

Figure 9 shows the effect of subtracting the background signal due to edge from data obtained from a typical scan. Nearly complete suppression of the edge signal was obtained.

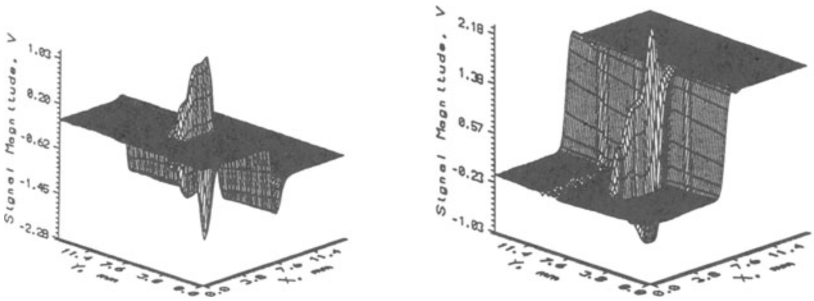

Horizontal Channel

Vertical Channel

Fig. 6. 2-D scan of notch 'A' (parallel orientation).

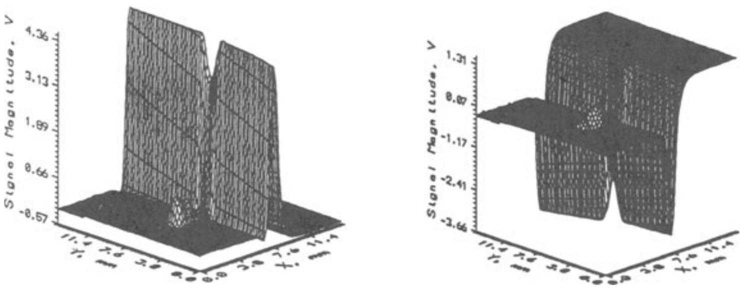

Horizontal Channel

Vertical Channel

Fig. 7. 2-D scan of notch 'A' (perpendicular orientation).

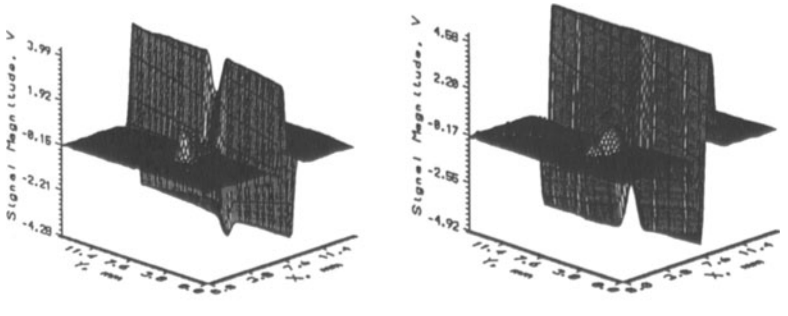

Horizontal Channel Vertical Channel

Figure 8. 2-D scan of notch 'A' with backing plate (perpendicular orientation).

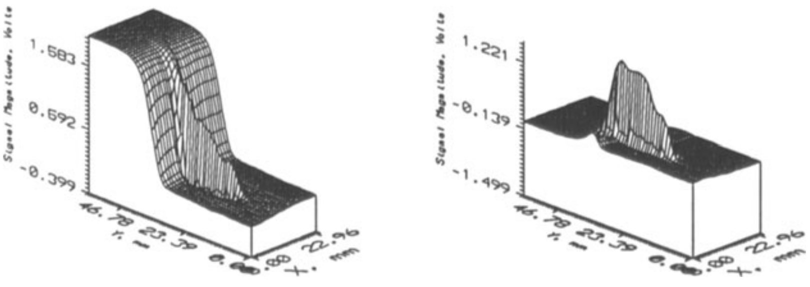

Raw data Processed data

Figure 9. Background subtraction.

SUMMARY

We have studied various aspects related to the detection of flaws at edges. A boundary element method (BEM) approach was used to model the signal due to the edge and was validated by comparison with experimental measurements. The influence on edge signals of frequency of operation, absolute or differential modes of probe operation, and of probe orientation for differential probes were investigated experimentally. Techniques such as signal processing and use of a backing plate were studied for their effectiveness in reducing the interfering effects of edges on flaw signals.

ACKNOWLEDGMENT

This work was sponsored by NIST under cooperative agreement #70NANB9H0916 and was performed at the Center for NDE, Iowa State University.

REFERENCES

1. N. Nakagawa and J. Chao, this volume.
2. J. Chao, D. Lehther, J.C. Moulder, and N. Nakagawa, this volume.
3. B. A. Auld, in *Eddy-Current Characterization of Materials and Structures*, ASTM STP 722, G. Birnbaum and G. Free, eds., p. 332 (1981).